

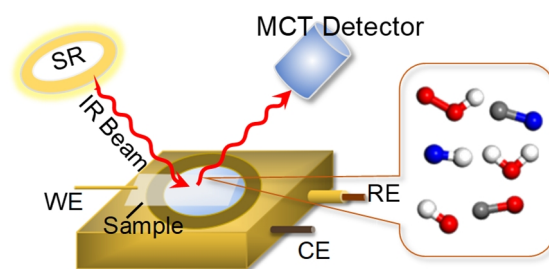
# In-Situ Synchrotron Radiation Infrared Spectroscopic Identification of Reactive Intermediates over Multiphase Electrocatalytic Interfaces

Wanlin Zhou<sup>1</sup>, Jingjing Jiang<sup>1</sup>, Weiren Cheng<sup>1</sup>, Hui Su<sup>1\*</sup> and Qinghua Liu<sup>1\*</sup>

<sup>1</sup>National Synchrotron Radiation Laboratory, University of Science and Technology of China, Hefei 230029, China

**ABSTRACT** A comprehensive understanding of the microscopic reaction mechanisms at the gas-solid-liquid electrochemical interfaces is urgently required for the development of advanced electrocatalysts applied in burgeoning sustainable energy conversion systems. In-situ synchrotron radiation Fourier transform infrared (SR-FTIR) spectroscopy is one of the most powerful techniques for investigating the evolving dynamics of reactive intermediates during electrocatalytic reactions. In this review, we methodically summarize the recent progress in the research of dynamic mechanisms for valuable electrocatalytic reactions based on in-situ SR-FTIR methodology. Moreover, the merits and drawbacks of SR-FTIR spectroscopy, the design principles of infrared beam setups and in-situ cells, as well as the in-situ measurement criteria are also discussed in detail. Lastly, the potential challenges and opportunities in this field are prudently stated. This review is expected to stimulate a broad interest in the material science and electrochemistry communities for exploring the dynamic mechanisms of prominent catalysis at the atomic/molecular level by using SR-based spectroscopy.

**Keywords:** synchrotron radiation, infrared spectroscopy, in-situ, reaction dynamics



## INTRODUCTION

The ever-deteriorating energy crisis and environmental issues caused by the severe burning of fossil fuels have aroused global attention.<sup>[1-3]</sup> Renewable energy conversion devices, such as fuel cells and nitrogen conversion, have timely emerged as a viable strategy to get rid of the dependence on depleted fossil fuels.<sup>[4,5]</sup> However, the sluggish redox kinetics of the prominent gas-involved electrocatalytic reactions, such as oxygen evolution reaction (OER), oxygen reduction reaction (ORR), urea oxidation reaction (UOR), nitrogen reduction reaction (NRR), etc. are the great obstacle to the overall efficiency improvement of the energy devices.<sup>[6-8]</sup> To operate these critical reactions efficiently, rationally designed electrocatalysts with high-performance are urgently needed, which largely depends on the in-depth understanding of the essential dynamic reaction mechanisms on gas-solid-liquid interfaces during electrocatalytic process.<sup>[9,10]</sup> Unfortunately, the commonly employed methods such as theoretical simulation and static characterization of the electronic structures cannot directly capture the key intermediates (\*OH, \*O, \*OOH, etc.) as well as the real evolution of reactive structures under realistic operating conditions.<sup>[11-13]</sup> Therefore, by reason of the complexity of the bonding information on electrode interface and the discontinuity of the weak key intermediates signals, using cogent in-situ spectroscopic techniques to detect the dynamic evolution process of molecular structure is quite necessary but still a grand challenge.<sup>[14-16]</sup>

Infrared (IR) spectroscopy with high sensitivity to functional groups is well known as an important technique for the dynamic exploration of molecular structure.<sup>[17,18]</sup> In recent years, IR spectroscopy has been increasingly applied in the real-time identification of reactive structures during electrocatalytic process, but the

main obstacles are still the weak signals of the transient intermediates that are difficult to capture and the absorption interference of electrolyte solution.<sup>[19,20]</sup> To enhance the absorption signal of the intermediate molecules and improve the accuracy of infrared identification, a typical technique that can be used is the modified attenuated total reflection infrared (ATR-IR) spectroscopy, in which a thin electrolyte layer is formed to greatly reduce the strong absorption of aqueous solution.<sup>[21,22]</sup> More importantly, while weakening the water absorption interference, enhancing IR light intensity is the most effective strategy for extracting intermediates signal under electrochemical operating conditions.<sup>[23,24]</sup> Synchrotron radiation Fourier transform infrared (SR-FTIR) spectroscopy has been demonstrated as an attractive technique with high-brilliance light source for dynamic detections in complex aqueous medium, which provides the possibility for in-situ identification of the key functional-group during electrocatalytic reaction.<sup>[25-28]</sup> Inevitably, there are still some scientific problems that lie in the in-situ detection of SR-FTIR technology, like the inferior signal-to-noise ratio (SNR) and the overlapping absorption of oxygen-containing groups in IR fingerprint region.<sup>[29,30]</sup> Hence, it is urgent to systematically summarize the research progress based on the SR-FTIR technology and explore more effective operating strategies, so as to provide a reliable correlation between the active structure evolution and the activity for the design of advanced electrocatalysts.

In this mini-review, we would firstly introduce the fundamental understanding of the SR-FTIR technology for identification of the reactive species over gas-solid-liquid electrocatalytic interfaces during working conditions. Meanwhile, the infrared beam setups, the in-situ cells and the measurement principles are discussed. Subsequently, the essential research achievements of dynamic studies for various typical electrocatalytic reactions by

using in-situ SR-FTIR technology are systematically scrutinized. At the end of this review, the potential challenges and opportunities in the application of SR-based spectroscopy, and the exploration prospect of the practical electrocatalysts are carefully stated for better popularizing the splendid in-situ SR-based technologies under realistic operating conditions.

## n SR-FTIR SPECTROSCOPIC TECHNOLOGY FOR IN-SITU DETECTIONS

**SR-FTIR Spectroscopy.** Infrared (IR) spectroscopy can be tracked as the earliest dispersive spectrometers directed at the characterization of molecular structure.<sup>[31,32]</sup> It was not until the advent of the Fourier-transform Infrared (FTIR) spectroscopy in 1950 that a significant technical change occurred, in which the full collimating infrared beam is split into sub-beams with optical path retardation by Michelson interferometer, and then the Fourier transform of the interfere-signal is used to obtain high quality IR spectra.<sup>[33,34]</sup> Since then, FTIR spectroscopy has been widely used for qualitative and quantitative analysis in the fields of materials science. However, most of the studies were conducted by the conventional laboratory IR light sources (e.g. mercury lamp, Globars), and focused on the mid-infrared region ( $600\text{--}4000\text{ cm}^{-1}$ ) with mean signal-to-noise ratio (SNR) due to the low intensity and limited sensitivity of the thermal source.<sup>[35,36]</sup> For the electrochemical systems with heterogeneous interfaces, the IR detection is more complicated because of the insurmountable strong interference of various species to infrared signals.

Synchrotron radiation (SR) is a type of electromagnetic radiation emitted when free electrons travel in a circular motion at high speed.<sup>[37]</sup> The SR-based Infrared spectroscopy (SR-FTIR) with unique spectral absorption properties has become a powerful technique superior to the conventional thermal source for the exploration of complex electrochemical systems.<sup>[25,38]</sup> The high brilliance is a well-known strength of SR-FTIR spectroscopy, which is extremely important for the SNR and sensitivity of IR investigations.<sup>[39,40]</sup> Generally, the SR light source can provide high-brilliance proton beams that are 2-3 orders of magnitude brighter than conventional thermal sources as the microscope aperture size is cut down to several micrometers scale, which provides an

assurance for the infrared detection with high SNR at micro-zone.<sup>[41-43]</sup> It is worth noting that the highly polarized light and the picosecond time scale of light pulses provided by the SR light source enable the detection of molecular structure to maintain class resolutions within a satisfactorily short acquisition time, even near the diffraction limits.<sup>[44,45]</sup> The wide photon flux extending from X-ray to the whole infrared region (covering near IR, middle IR and far IR) is another particular merit of SR source.<sup>[46]</sup> In principle, the species evolution measurement on electrochemical interfaces is mainly achieved by the IR spectrum that identifies the changes in dipole moment of the surface molecules or groups at the middle IR range.<sup>[17,47,48]</sup> The SR-FTIR spectroscopy has incomparable sensitivity and high-resolution in the detection of molecular dipole moment changes and unique functional group structures, which makes it an indispensable implement for the detection of intermediate species during the electrochemical reaction interface.<sup>[49,50]</sup> Typically, the SR apparatus with the customized infrared spectrum line and the specialized spectro-microscopy has the technical strength to output persistent and stable electron/optical beams, which is the solid foundation for the high-quality FTIR spectrum acquisition.<sup>[39]</sup>

**Acquisition of In-Situ SR-FTIR Spectroscopy.** Great efforts have been made to develop effective infrared measurement methods, including Transmission,<sup>[51]</sup> Diffuse-Reflectance (DRIFTS),<sup>[52]</sup> Attenuated Total Reflection (ATR)<sup>[53]</sup> and other Reflection-Absorption (RAIRS)<sup>[54]</sup> modes, which are genuinely approved for acquisition of the infrared spectroscopy feedback signals. Among them, ATR mode as well as the derived surface-enhanced infrared (ATR-SEIR) is the most common approaches, especially for the infrared collection on electrochemical multiphase interfaces (Figure 1a). ATR-IR is an effective internal reflection IR in-situ measurement mode, and the multiple-bounce ATR-IR is more widely used than the single-bounce to obtain stronger signals. The complexity of the electrochemical interfaces is the huge obstacle of infrared detection because the infrared adsorption of the reactive species (oxygen-related species,  $800\text{--}1500\text{ cm}^{-1}$ ; hydrogen-related species,  $3000\text{--}4000\text{ cm}^{-1}$ ) is highly overlapped with the strong absorption region of water molecules in the liquid media.<sup>[55-57]</sup> Although many feasible measures such as optimizing optical pathway, adjusting the windows configuration, etc. are implemented in ATR-IR setups to enhance the intensity of collectible infrared signal in disturbing environment, there is no super-order-of-magnitude signal enhancement, which instead increases the risk of noises and sacrifices some actual conditions of the electrocatalytic reactions.<sup>[22,58,59]</sup>

The high brightness of SR-based light source can easily realize the signal acquisition in single-reflection mode (Figure 1b), which greatly reduces the noise and uncertainty caused by the multi-reflection of conventional light source.<sup>[17]</sup> The acquisition principle of the single-reflection mode for SR-FTIR spectroscopy is shown in Figure 1b. The SR infrared beam irradiates the sample plane through the ZnSe window at a specific angle, and the feedback signal is directly collected by the mercury-cadmium-telluride (MCT) detector only after one reflection.<sup>[60]</sup> It should be concerned that the incident angle is best kept at  $83\text{--}88^\circ$ , which is based on the Greenler's calculation,<sup>[36]</sup> resulting in the strongest absorption

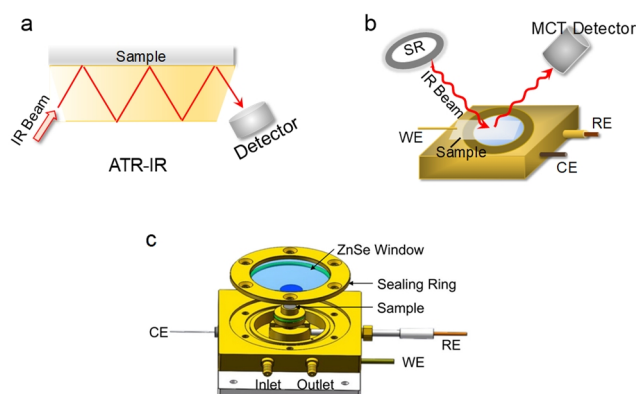


**Figure 1.** Schematic illustration of (a) ATR-IR, (b) SR-IR spectroscopy and (c) decomposing diagram of in-situ SRIR cell. Reproduced with permission,<sup>[19]</sup> copyright 2020, Elsevier.

of infrared signal and the high quality SNR. The critical value of the incident angle ( $\theta$ ) can be determined by the ratio of the refractive indices of the sample ( $n_2$ ) and the internal reflection element (ZnSe,  $n_1$ ). The depth at which the light intensity attenuated to  $1/e$  in the sample is the effective penetration depth ( $d_p$ ) of the IR beam, and  $d_p$  is related to the light wavelength ( $\lambda$ ), the incident angle ( $\theta$ ) and the refractive index:

$$d_p = \frac{\lambda}{2\pi n_1 (\sin^2 \theta_i - (n_2/n_1)^2)^{1/2}}$$

A typical home-made cell for in-situ SR-FTIR investigations is schematically exhibited in Figure 1c. To reduce the interference of surface water absorption, the carbon cloth ( $1 \times 1 \text{ cm}^2$ ) coated with catalysts is tightly closed to the substrate of glass carbon wafer, where the water film on the surface of porous working electrode is maintained in micron-level thickness ( $\sim 5 \text{ }\mu\text{m}$ ) by the capillarity permeation of electrolyte solution. Moreover, the height of the glassy carbon substrate and the tightness of the ZnSe window seals are adjustable. The diffusion efficiency of reactive species in electrolyte is a critical part in the in-situ SR-FTIR measurements. For this home-made in-situ cell, the electrolyte in the cell chamber is dynamically circulated from the inlet to the outlet of the cell by a peristaltic pump and an external reservoir.<sup>[19]</sup>

In-situ SR-FTIR measurement in the electrochemical systems is an extremely delicate project. On the basis of optimizing the SR-IR beam setups and in-situ reaction cells, there are some pivotal issues that need to be considered during the IR signal acquisition. The focus of infrared beam on catalyst sample is the primary challenge of in-situ measurement. To ensure that the feedback infrared signal for the target sample is collected, reference signals under different ex-situ conditions require to be gathered and compared, including the two states of “with and without ZnSe window”, the absence of electrolyte, and after circulating electrolyte situations. Then, the focus accuracy of IR beam can be judged based

on the changes of signal curves under different conditions. In-situ electrochemical measurement is achieved by applying potential step by step. The accurate recording of the intermediate molecules at a given potential is recommended after the potential has been applied for a period of time ( $\sim 15 \text{ min}$ ) and the working electrode surface has reached a quasi-static state. The acquisition parameters such as scan number and step interval are closely related to the SNR of the data, which are usually selected as 514 scans at the interval of  $2 \text{ cm}^{-1}$ . Repeated measurements (2-3 times) for the same sample are suggested to ensure that the IR spectra reflect the accurate evolution information during the reaction process.

## n MONITORING REACTIVE INTERMEDIATES OF ELECTROCHEMICAL INTERFACE BY IN-SITU SR-FTIR SPECTROSCOPY

With the deepening of research, in-situ infrared spectroscopy has been developed from the initial detection of oxygen- or hydrogen-related species on the metal or metal oxide surface to the in-situ accurate identification of C-, N-, O- and H-related species over multiphase electrochemical interfaces.<sup>[61,62]</sup> The in-situ exploration of the key reactive species in electrochemical reactions has triggered a series of pioneering researches in advanced materials science.<sup>[63,64]</sup> In this section, the main application advances of the in-situ SR-based FTIR techniques in electrochemical energy conversions fields are systematically described according to the reaction types.

**OER.** The complex multi-proton and electron transfer steps of oxygen evolution reaction ( $2\text{H}_2\text{O} \rightarrow 4\text{H}^+ + 4\text{e}^- + \text{O}_2$ ) is the bottleneck of improving the overall efficiency of energy conversion and storage devices.<sup>[65,66]</sup> The generation of the key intermediates and their elusive interaction with the active sites in OER process are regarded as the crucial issues to enhance the reaction rate. And

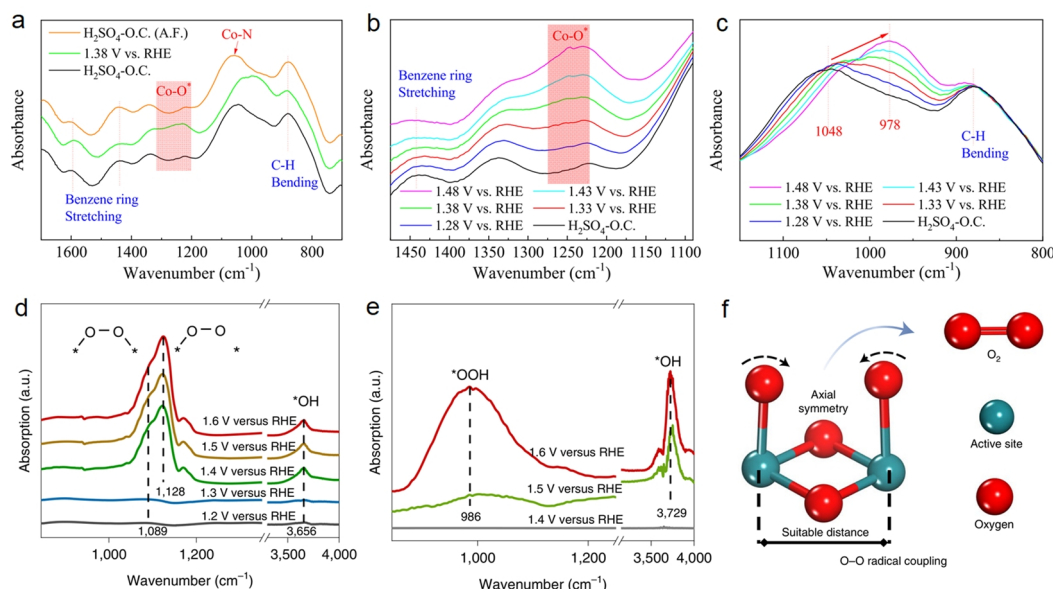


**Figure 2.** a-c, In-situ SR-FTIR signals for Co active sites under realistic OER operation conditions. Reproduced with permission.<sup>[69]</sup> Copyright 2019, American Chemical Society. d-e, In-situ SR-FTIR signal for 12Ru/MnO<sub>2</sub> samples (d) and RuO<sub>2</sub> reference catalysts (e). f, Diatomic active sites with suitable spacing facilitate the O-O radical coupling. Reproduced with permission.<sup>[70]</sup> Copyright 2021, Nature Publishing Group.

numerous studies have been carried out through the experimental exploration and theoretical simulation.<sup>[67,68]</sup> In this regard, the SR-FTIR technology, which specializes in capturing transient species over heterogeneous reaction interfaces, has become an indispensable enabler for electrocatalytic dynamics studies.

How to achieve high activity and long-term durability of OER in acidic electrolytes is an urgent scientific problem to be solved in the field of electrocatalyst exploration. To this end, thoroughly understanding the catalytic mechanism of acid-resistant OER electrocatalysts under realistic working conditions is an effective solution. Liu group firstly performed in-situ SR-FTIR spectroscopy to investigate the acidic OER catalytic mechanism of hetero-N-coordinated active metal sites ( $\text{H}_2\text{N-Co-N}_x$ ) in homemade electrochemical cells.<sup>[69]</sup> Under  $\text{H}_2\text{SO}_4$ -impregnated open-circuit conditions, excluding the benzene ring and C-H vibrations, only the distinct absorption band at  $\sim 1048\text{ cm}^{-1}$  attributed to Co-N can be observed (Figure 2a). With the potential applied under the in-situ operation conditions, a newly formed potential-dependent vibration band at  $1248\text{ cm}^{-1}$  appears when the potential is greater than  $1.38\text{ V}$ , implying that the effective formation of  $\text{*O}$  intermediates over Co metal sites forms the reactive center of  $\text{H}_2\text{N-(*O-Co)-N}_4$  (Figure 2b). Meanwhile, during the in-situ operation process, the absorption vibration of Co-N bond undergoes a significant redshift that varies with the applied voltage (moving from  $1048$  to  $978\text{ cm}^{-1}$ ) (Figure 2c). This phenomenon reveals an active electron transfer from the metal center to the surrounding N atoms with the potential fluctuations, which apparently favors the active sites  $\text{H}_2\text{N-(*O-Co)-N}_4$  following a rapid OER kinetics in acidic electrolytes. Similar in-situ SR-FTIR studies were also carried out on metal-free amino-rich carbon-based ( $\text{H}_2\text{N-C=C}$ ) sites.<sup>[71]</sup> The regular

changes in the characteristic vibration of C-O\* and C-N bonds during SR-FTIR testing of acidic OER demonstrate the electron transfer from C to the  $\text{NH}_2$  group. Meaningfully, the electron transitions favor the emergence of  $\text{*O}$  on amino-HNC to form the  $\text{H}_2\text{N-(*O-C)-C}$  active sites, which contributes to a high-efficient reaction process. The acidic OER multi-electron transfer pathway was investigated by Lee et al. through employing in-situ SR-FTIR spectra technology.<sup>[70]</sup> For the well-designed  $\alpha\text{-MnO}_2$  nanofiber-supported Ru catalyst samples ( $12\text{Ru/MnO}_2$ ), the absorption vibration dramatically increased, which can be assigned to the accumulation of  $\text{*O-O}$  intermediates (Figure 2d). For comparison, the SR-FTIR measurement of  $\text{RuO}_2$  reference catalyst typically reveals the traditional Ru-OOH active intermediates and the rate-limiting step intermediate of  $\text{*OH}$  (Figure 2e), which suggests the conventional evolution mechanism of OER pathway. Combining with DFT simulations, it can be concluded that the reconstructed Ru atom array on  $\alpha\text{-MnO}_2$  nanofiber can catalyze OER to follow an efficient kinetic mechanism of direct O-O radical coupling (Figure 2f), which successfully overcomes the overpotential limitations lying in conventional multiple intermediate mechanism.

Single-atom catalysts have been widely adopted to in-depth investigate the reaction mechanism of electrocatalytic interface due to their atomically dispersed metal active sites. For example, Yao and coworkers systematically investigated the intrinsic catalytic activity and stability on atomically  $\text{Ru}_1\text{-N}_4$  site involved catalysts.<sup>[72]</sup> In-situ SR-FTIR characterization strategy plays a crucial role in the identification of key intermediates during the reaction process. For the in-situ SR-FTIR measurements in Figure 3a-b, a newly formed absorption band appeared at  $\sim 764\text{ cm}^{-1}$  after the higher operating potential of  $1.5\text{ V}$  was applied, and gradually disap-

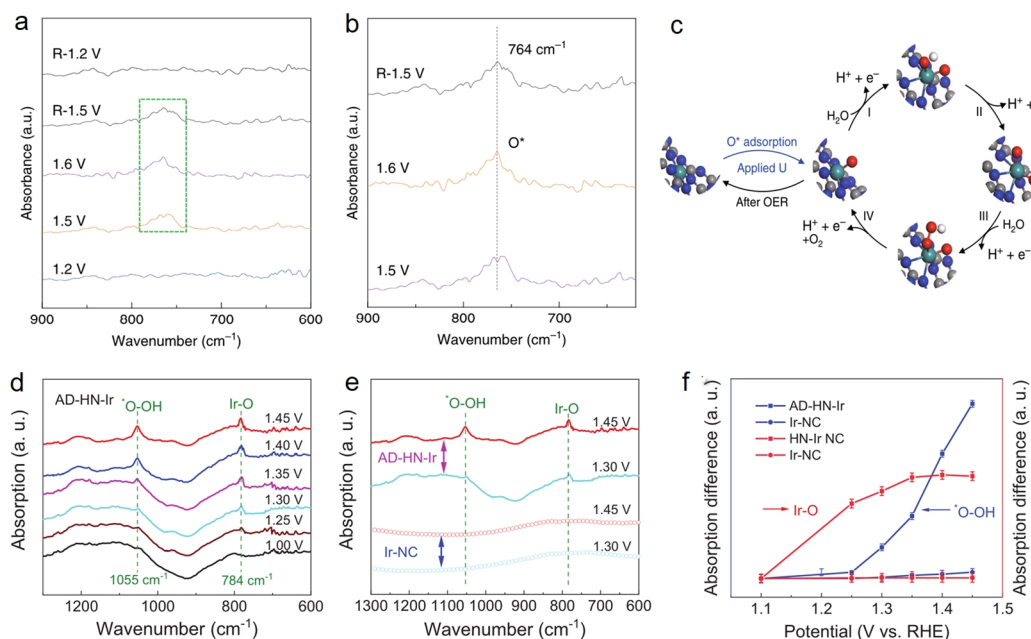


**Figure 3.** In-situ SR-FTIR measurements under acidic OER conditions for Ru-N-C (a) and the enlarged image of the area  $\sim 764\text{ cm}^{-1}$  (b). c, OER mechanism for Ru-N-C. Reproduced with permission.<sup>[72]</sup> Copyright 2019, Nature Publishing Group. d-e, In-situ SR-FTIR measurements for AD-HN-Ir under acidic OER conditions. d, and for AD-HN-Ir and Ir-NC catalyst under representing potentials (e). f, Contrast of vibration intensity. Reproduced with permission.<sup>[73]</sup> Copyright 2021, Nature Publishing Group.



peared after reversing the potential from 1.6 to 1.2 V. This valuable phenomenon of reversible adsorption and desorption of reactive species strongly demonstrates the evolution of  $^*\text{O}$  intermediates at single atomic Ru sites. As can be seen in Figure 3c, the dynamic formed O-Ru<sub>1</sub>-N<sub>4</sub> site by  $^*\text{O}$  adsorption is the first activation step for OER, which then tends to undergo the nucleophilic attack reaction and deprotonate to produce  $^*\text{OOH}$ . Combined with theoretical calculations, the high oxidation state of O-Ru<sub>1</sub>-N<sub>4</sub> was demonstrated to be formed by the pre-adsorption of single oxygen under realistic reaction state, which provides a low O-O coupling barrier for the formation of  $^*\text{OOH}$  key intermediates in OER process. A more in-depth investigation on the evolution of reactive single sites was carried out by Liu group.<sup>[73]</sup> Through aminating (-NH<sub>2</sub>) the benzenoid-amine group on the carbon substrate, the atomically dispersed iridium atoms were then anchored uniformly by the uncoordinated N atoms to form the active hetero-Ir-N<sub>4</sub> structure. During the catalytic OER process, in-situ SR-FTIR measurements reveal that the Ir-O unit vibration appeared first at 784 cm<sup>-1</sup> of 1.25 V and the vibration of  $^*\text{OOH}$  emerged at 1055 cm<sup>-1</sup> after the potential of 1.35 V was applied (Figure 3d). By comparing with the reference catalyst in Figure 3e, no obvious vibration band can be observed for Ir-NC, suggesting that the pre-formed Ir-O structure (784 cm<sup>-1</sup>) for AD-HN-Ir catalyst is able to accelerate the generation of  $^*\text{OOH}$  intermediate. The favorable relationship between Ir-O and  $^*\text{OOH}$  intermediates was assessed by the analysis of the absorption intensity (Figure 3f). The strong dynamic coupling between the hetero-Ir-N<sub>4</sub> structure and oxygen atom occurs at the initial potential of 1.25 V for OER, which effectively forms the O-hetero-Ir-N<sub>4</sub> active site with high-valence state, thus significantly promoting the generation of reaction intermediate  $^*\text{OOH}$  and accelerating the acidic OER kinetics.

**ORR.** Oxygen reduction reaction (ORR) is the most widely studied topic in the fields of electrochemistry and catalysis, but its reaction mechanism is still elusive due to the diversity and complexity of the reaction process.<sup>[74,75]</sup> In addition to the multi-electron transfer included reaction pathway with water as the final product, the two-electron reaction pathway with oxygen reduced to peroxide ions ( $\text{HO}_2^-$ ) is also prone to occur. Thus, highly selective ORR catalysts are required to ensure the reaction efficiency of the single pathway, which in turn relies on a thorough understanding of intrinsic reaction mechanism. Liu group took uniformly dispersed single metal site catalysts as an example to comprehensively explore the dynamic mechanism between crucial reactive intermediates and catalytic active structures in the ORR process.<sup>[28]</sup> During the in-situ SR-FTIR measurement for Ni<sub>1</sub>-NC (Figure 4a), the infrared vibration located at 906 cm<sup>-1</sup> of Ni-O\* emerged after the ORR operating potential was applied and the intensity gradually increased. The difference of vibration for the detected O-H band located at 3465 cm<sup>-1</sup> shows an increase in intensity prior to Ni-O\* and a slight decrease after applying 0.80 V (Figure 4b). In-situ SR-FTIR was conducted by using isotope-labeling strategies to clarify the source of O atom in O-H and  $^*\text{O}$  species and further analyze the relationship between the intermediates. A clear red-shift can be observed for the Ni-O\* vibration when replacing <sup>16</sup>O<sub>2</sub> gas with <sup>18</sup>O<sub>2</sub> (Figure 4c), and in the meanwhile, the O-H vibration remains the location of 3465 cm<sup>-1</sup> (Figure 4d), collectively implying that the  $^*\text{O}$  intermediate in ORR process originates from adsorbed O<sub>2</sub> and O-H species derived from H<sub>2</sub>O. In conclusion, the  $^*\text{OH}_2$  molecule coupled with  $^*\text{O}_2$  precursor over Ni active center naturally accelerates the generation of metastable  $^*\text{O-Ni}_1\text{N}_2$  configuration. The single-atom Fe sites dispersed samples have also been used as model electrocatalysts for the in-situ SR-FTIR studies

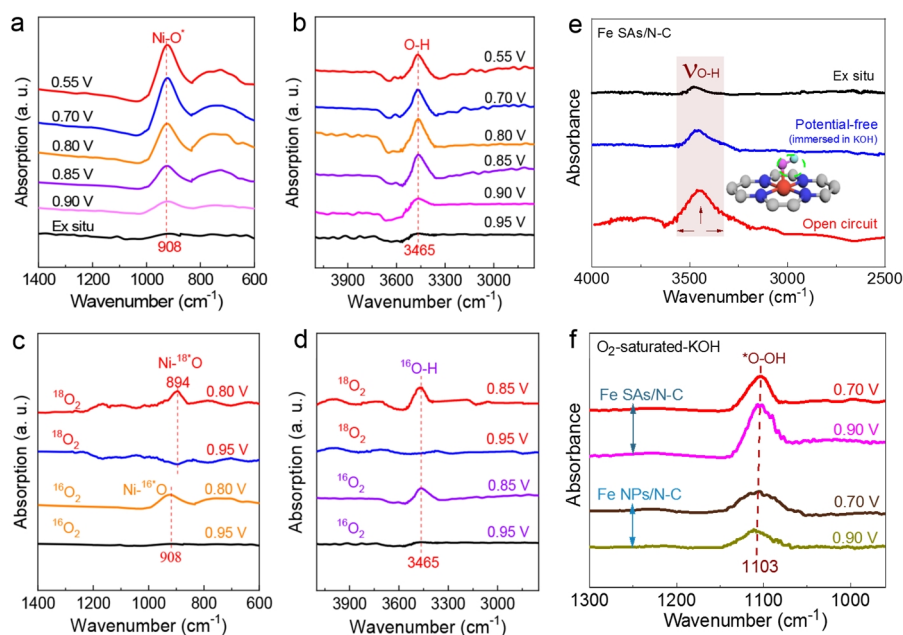


**Figure 4.** a-b, In-situ SR-FTIR measurements under alkaline ORR conditions for Ni<sub>1</sub>-NC. c-d, Isotope-labeling operando SR-FTIR measurements under alkaline ORR conditions for Ni<sub>1</sub>-NC. Reproduced with permission.<sup>[28]</sup> Copyright 2020, American Chemical Society. e, SR-FTIR measurements under various conditions. f, In-situ SR-FTIR measurements under alkaline ORR conditions. Reproduced with permission.<sup>[12]</sup> Copyright 2021, American Chemical Society.

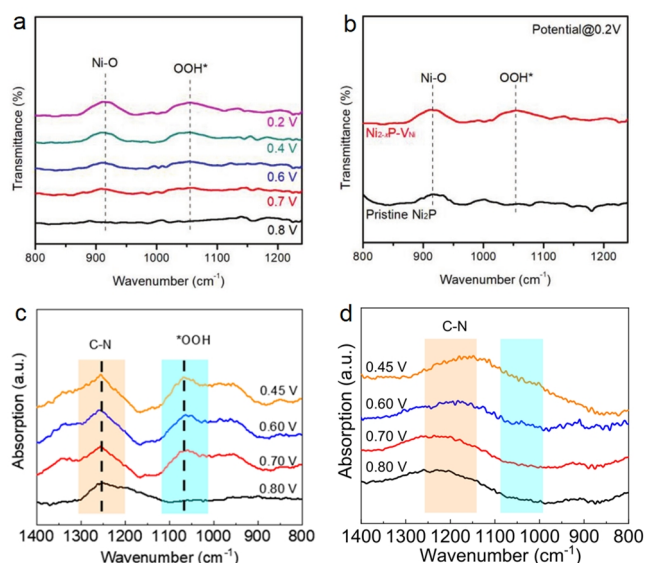


**Figure 5.** a, In-situ SR-FTIR spectra under ORR operating conditions for  $\text{Ni}_{2-x}\text{P-V}_{\text{Ni}}$ . b, SR-FTIR spectra under ORR operating potentials of 0.2 V for  $\text{Ni}_{2-x}\text{P-V}_{\text{Ni}}$  and pristine  $\text{Ni}_3\text{P}$ . Reproduced with permission.<sup>[76]</sup> Copyright 2022, Wiley-VCH GmbH. c and d, In-situ SR-FTIR spectra under ORR operating conditions for Br-Ni MOF (c) and Ni MOF (d). Reproduced with permission.<sup>[77]</sup> Copyright 2021, American Chemical Society.

by Liu group.<sup>[12]</sup> For the Fe SAs catalysts, an O-H vibration was detected by in-situ SR-FTIR measurement under OCV conditions (Figure 4e), which indicates the hydroxyl species (-OH) pre-adsorption over the Fe active center ( $\text{HO-Fe-N}_2$ ). The crucial \*O-OH intermediate begins to accumulate after the ORR potential is applied and shows obvious decline in intensity as the potential drops from 0.90 to 0.70 V, which is different from the SR-FTIR measurement results with no noticeable changes of \*O-OH vibration for Fe NPs reference samples (Figure 4f). Notably, the investigation of the characteristic vibration (Fe-OH, \*OOH) shows that the Fe-OH active unit tends to be stable after 0.9 V, while the \*OOH intermediates accumulate rapidly before 0.9 V and then effectively cleavage, implying the preformed  $\text{HO-Fe-N}_2$  structure is the power center to accelerate the generation and continuous cleavage of \*O-OH intermediates. This optimized mechanism by dynamic activating of catalytic sites paves the way of 4 e<sup>-</sup> ORR going kinetic-accelerated steps.

The ORR reaction process following 2e<sup>-</sup> pathway has also been deeply studied using in-situ SR-FTIR techniques. Zhao and coworkers reported the 2e<sup>-</sup> ORR mechanism during the solid-liquid reaction interface for Ni vacancies enriched phosphide model catalysts by studying the evolution of reaction intermediates.<sup>[76]</sup> For the in-situ measurement on  $\text{Ni}_{2-x}\text{P-V}_{\text{Ni}}$  (Figure 5a), a gradual increase in the coordination of the oxygenated species with the Ni sites was observed during catalysis process, as the vibration assigned to Ni-O at 916 cm<sup>-1</sup> was inversely enhanced with decreasing the cathodic potential. More importantly, the O-O stretching within \*OOH intermediate located at 1060 cm<sup>-1</sup> rises continuously with the ORR potential applied, which confirms that the cleavage of \*OOH species is suppressed and favors a high

selectivity for the 2e<sup>-</sup> process towards  $\text{H}_2\text{O}_2$ . The pristine  $\text{Ni}_2\text{P}$  was tested by SR-FTIR for proving the vital function of Ni cationic vacancies ( $\text{V}_{\text{Ni}}$ ). As expected, there was no distinct characteristic vibration (\*OOH) under all the in-situ tested potentials (Figure 5b). Thus, the active vacancies within  $\text{Ni}_{2-x}\text{P-V}_{\text{Ni}}$  catalysts are likely to facilitate the generation of \*OOH and restrain its decomposition, which effectively improves the reaction selectivity of  $\text{H}_2\text{O}_2$ . The selectivity of the ORR for 2e<sup>-</sup> process was inspected by Liu group on the halogen confined Ni MOF materials (X-Ni MOF).<sup>[77]</sup> Suppressing the cleavage of \*OOH species during multi-steps of ORR is the key to the production of  $\text{H}_2\text{O}_2$ , which is likely to be achieved by the lattice contraction involved X-Ni MOF because of its low-spin electron configuration. The in-situ SR-FTIR was employed to probe the actual reaction at the solid-liquid interface and the results in Figure 5c, d were obtained. Different from the undulating C-N vibrations that always present during the in-situ operation process, the absorbed vibration at 1070 cm<sup>-1</sup> of \*OOH superoxide species can be observed only after the low potential of 0.70 V was applied. And the absence of detectable \*OOH vibrations on Ni MOF under all potentials demonstrates the competence of Br-Ni MOF to accumulate \*OOH at the catalytic interface (Figure 5d). Accordingly, the self-confined Br anions in Ni MOF with adequate nanocavity are the pivotal role for boosting  $\text{H}_2\text{O}_2$  production by accumulating \*OOH on catalytic sites.

**Urea-Related Reactions (UOR/NRR).** The urea oxidation reaction and its reverse reaction involving multiple restricted procedures and complicated intermediates are of great significance in the field of energy electrochemistry, but suffer from even more sluggish kinetics and ultrahigh overpotential than OER/ORR because of its six-electron-proton (or hydroxyl) coupled transfer process.<sup>[78,79]</sup> Exploitation of competent catalysts through comprehensive understanding of reaction pathways and mechanisms for the untoward UOR/NRR is of impendency but still poses significant challenges. At this stage, in-situ SR-FTIR methodology assumes a critical assignment in the capture of reactive intermediates during realistic reaction process. Qiao group prepared a typical nickel ferrocyanide electrocatalyst ( $\text{Ni}_2\text{Fe}(\text{CN})_6$ ) to trigger the UOR favoring a pathway including two main procedures with ammonia species as the intermediate, which are highly efficient than the conventionally understood mechanisms that are difficult to proceed.<sup>[80]</sup> The in-situ SR-FTIR technique has played a crucial role in identifying the key intermediates (\* $\text{N}=\text{NH}_2^+$ , \* $\text{OCONH}_2$ ) of rate-limiting reactions during two-procedure pathway. Compared with only three peaks representing  $\text{CO}_2$ , C=O (1700 cm<sup>-1</sup>) and N-H (1650 cm<sup>-1</sup>) under OCP condition (Figure 6a), two potential-dependent vibration peaks at 2925 and 1203 cm<sup>-1</sup> were added under operating potentials (1.35-1.65 V). Notably, the absorption signal which becomes progressively stronger as the operating potential increases at 2925 and 1203 cm<sup>-1</sup> is derived from the vibration of N-H band in \* $\text{N}=\text{NH}_2^+$  intermediate species and the vibration of C-O band in \* $\text{OCONH}_2$  species, respectively. According to the universally accepted mechanism of UOR, the \*CON, \*CO-NH and \*COO are the key intermediates associated with rate-determining steps (RDS) which have not been detected for the  $\text{Ni}_2\text{Fe}(\text{CN})_6$  electrocatalyst in in-situ SR-FTIR spectra, suggesting the  $\text{Ni}_2\text{Fe}(\text{CN})_6$  catalytic urea oxidation follows a diverse pathway.

The in-situ SR-FTIR analysis was also conducted for the  $\text{NiC}_2\text{O}_4$  catalyst as a reference (Figure 6b), and the special characteristic vibrations of N-H in  $^*\text{N}=\text{NH}_2^+$  and C-O in  $^*\text{OCONH}_2$  were not observed. Moreover, a significant absorption vibration of  $\text{CNO}^-$  appears at  $2,136\text{ cm}^{-1}$ , which is consistent with the universal reaction mechanism of UOR. At this stage, the  $\text{Ni}_2\text{Fe}(\text{CN})_6$  electrocatalyst catalyzes UOR with more beneficial kinetic energetics with a chemical process for ammonia production at the Ni site, followed by an electrochemical process for ammonia decomposition to  $\text{N}_2$  at the Fe site (Figure 6c).

Urea is one of the indispensable nitrogenous fertilizers for the survival and development of human society. However, its synthesis still faces great challenges with harsh conditions and complex processes.<sup>[81-83]</sup> Based on this scientific question, PdCu nanoalloy electrocatalyst with  $\text{TiO}_2$  nanosheets as support was prepared by Wang et al.<sup>[84]</sup> to realize direct generation of the C-N bond by the  $^*\text{N}=\text{N}^*$  and CO produced by spontaneous reaction of  $\text{N}_2$  and  $\text{CO}_2$  in aqueous solution. The in-situ SR-FTIR was employed to monitor the evolution of pivotal chemical bonds during the catalytic reaction process. The characteristics of vibration at  $3171$ ,  $3291$  and  $3441\text{ cm}^{-1}$  associated with the generation of  $\text{NH}_2$  and  $\text{NH}$  species appeared after the driving potential of  $-0.20\text{ V}$  was applied (Figure 7a), suggesting no electro-reduction of  $\text{N}_2$  and  $\text{CO}_2$  occurred under low potential ( $-0.15\text{ V}$ ). And the  $\text{CO}_2$  reduction was found slowly under  $-0.25\text{ V}$  with the emergence of C=O and C-O vibrations at  $1699$ ,  $1177$  and  $1314\text{ cm}^{-1}$  (Figure 7b).

The origin of N and C elements was tracked by isotopic-labeling in-situ SR-FTIR. As seen from Figure 7c, d, all the vibrations ( $\text{NH}_2$ ,  $\text{NH}$ , C=O and C-N) were shifted by more than  $20\text{ cm}^{-1}$  when the isotopically labeled  $\text{N}_2$  and/or  $\text{CO}_2$  were replaced, confirming that the  $\text{N}_2$  and  $\text{CO}_2$  feeding gases were involved during the electro-reduction reaction. The validation experiments of in-situ SR-FTIR

tests on  $\text{TiO}_2$ -400 matrix show that no significant infrared signals of intermediate species were observed, verifying that PdCu alloy is the catalytic active structure. Throughout the whole reaction process with  $\text{N}_2$  and  $\text{CO}_2$  as raw materials,  $\text{N}_2$  is activated at low potential to generate  $^*\text{N}_2$ , which is able to promote the reduction of  $\text{CO}_2$  to CO and in turn alliance with  $^*\text{N}_2$  to form the C-N bond that is crucial for urea synthesis reaction.

For the urea production, an indium hydroxide electrocatalyst was reported to achieve direct electrochemical coupling of  $\text{CO}_2$  with  $\text{NO}_3^-$ , which takes advantage of the low energy barrier on  $\{100\}$  facets that proceed the key stages of the C-N bond formation in urea synthesis process.<sup>[62]</sup> The in-situ SR-FTIR measurement justifies the  $^*\text{CO}_2\text{NH}_2$  intermediate protonated into  $^*\text{COOHNH}_2$  in the rate-determining step under the proposed catalytic mechanisms. This work makes it possible to achieve effectively C-N coupling via  $\text{NO}_3^-$  and  $\text{CO}_2$  excitation at mild conditions.

**HER.** Hydrogen evolution reaction (HER) is an important cathode semi-reaction in water electrolysis industry. The potential two individual reaction pathways (Heyrovsky/Tafel steps) have extremely hindered the advance of water-electrolytic hydrogen making equipment.<sup>[85]</sup> The HER process starts with the Volmer steps of the proton depletion, and the subsequent hydrogen desorption process may go through two reaction pathways: the electro-desorption of adsorbed hydrogen atom (Heyrovsky step) or the proton recombination (Tafel step).<sup>[86]</sup> Moreover, the Volmer step in acidic electrolytes undergoes the depletion protons, whereas in alkaline electrolytes the decomposition of water molecules occurs first. The dynamic mechanism of the reactive intermediates in both acidic and alkaline electrolytes during HER process was first investigated in detail by Li et al. by using in-situ SR-FTIR methodology.<sup>[87]</sup> For acidic HER, the dynamic evolution of protons was

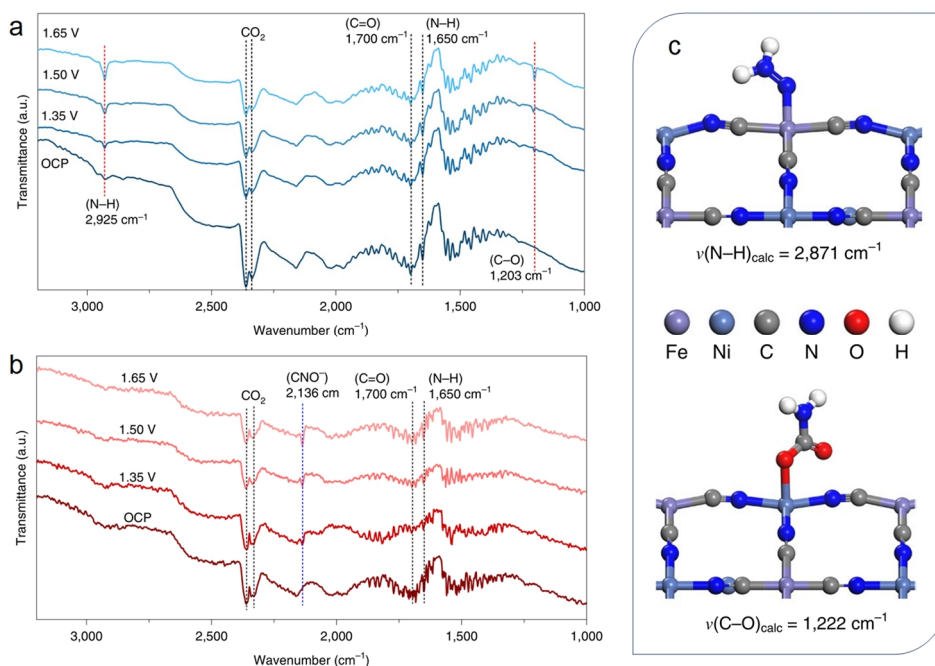


**Figure 6.** In-situ SR-FTIR spectra under UOR operating conditions for  $\text{Ni}_2\text{Fe}(\text{CN})_6$  (a) and  $\text{NiC}_2\text{O}_4$  (b). c, the harmonic vibrational models of the  $^*\text{N}=\text{NH}_2^+$  species on Fe site and the  $^*\text{OCONH}_2$  species on Ni site. Reproduced with permission.<sup>[80]</sup> Copyright 2021, Nature Publishing Group.

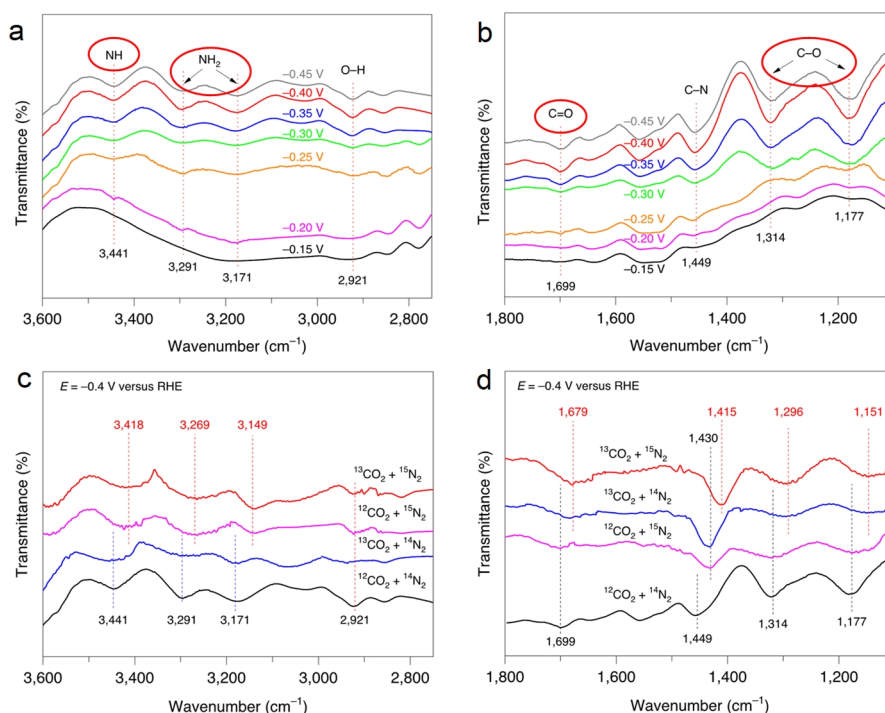


**Figure 7.** In-situ SR-FTIR spectra (a-b) and isotope-labelling testing (c-d) under the operating electroreduction conditions for Pd<sub>1</sub>Cu<sub>1</sub>/TiO<sub>2</sub>-400. Reproduced with permission.<sup>[64]</sup> Copyright 2020, Nature Publishing Group.

revealed by the emergent absorption vibration at around 1100 cm<sup>-1</sup>, which represents that the H atoms are adsorbed on the Ru site as the reaction intermediate (terminal H). The HER mechanism in alkaline electrolyte was also detected under realistic reaction conditions. The reaction continues with the intermittent potential applied, and the premier SRIR signal appeared at 1634 cm<sup>-1</sup>, representing the initial adsorption of H<sub>2</sub>O (H<sub>2</sub>O<sub>ad</sub>, δ<sub>H<sub>2</sub>O</sub>) in HER electrocatalysis process. Subsequently, a potential-dependent vibration at 1840 cm<sup>-1</sup> appeared, which was assigned to the adsorbed H derived from the decomposed H<sub>2</sub>O<sub>ad</sub>. After the Volmer steps which contain the adsorption and dissociation of H<sub>2</sub>O molecules into terminal OH and H, alkaline HER at the Ru site undergoes the Heyrovsky process, that is, the OH desorbs while the H<sub>ad</sub> recombines with adjacent H<sub>2</sub>O to release OH<sup>-</sup> and H<sub>2</sub>. Subsequently, the in-situ SR-FTIR methodology was widely used in the identification of reaction pathways and mechanism studies in the HER process.<sup>[88-90]</sup> Typically, in-situ SR-FTIR was used to identify active sites based on the sensitivity to light element species.<sup>[91]</sup> During SR-FTIR measurements for the as-designed catalyst, two obvious IR vibrations were observed at 1250 and 1120-1020 cm<sup>-1</sup>, belonging to the rich C-N and C-C stretching within the catalyst. The newly potential-dependent vibration was located at 1635 cm<sup>-1</sup> ranging from -10 to -70 mV, which was ascribed to the formation of N-\*H, indicating that the crucial \*H intermediate was generated over N active sites. This study is a bright inspiration for researchers to broaden the application scope of in-situ SR-FTIR methodology.

## n SUMMARY AND PERSPECTIVES

SR-FTIR spectroscopy has yielded abundant progress in reveal-

ing electrochemical reaction mechanisms through dynamic evolution studies of the adsorbed species. Several significant conclusions can be classified as follows: (1) The dynamic adsorption of oxygen species (oxygen atom or \*O intermediate) during abstruse acidic OER process may stimulate the kinetic activity of catalytic center, which is also expected to promote the direct coupling of O-O radicals and break the traditional mechanisms. (2) The unsaturated coordination metal sites (M-N<sub>2</sub>, HO-M-N<sub>2</sub>) formed during ORR process can serve as highly reactive centers for transition intermediates (\*O, \*OOH). (3) The \*N=NH<sub>2</sub><sup>+</sup> and \*OCONH<sub>2</sub> perform as the efficient intermediates for UOR with favorable thermal/kinetic energetics. (4) The terminal H (\*H) is identified as the crucial intermediate of Volmer step during HER process. These valuable results emphasize the significance of in-situ SR-FTIR spectroscopy technique in elucidating the intrinsic mechanisms of electrocatalytic reactions. Based on a careful analysis of the current research situation and advancements, we propose here some potential challenges and useful strategies for the future development of this technology in electrocatalytic fields.

(1) The spatial resolution of optical microscope can only reach tens of microns, which is limited by the diffraction limit under traditional infrared radiation. The SR-IR technology, based on the high brightness of synchrotron source, provides a promising opportunity for the high-SNR detection at the desirable micro-zone. Note that the tight coordination between the SR infrared optical systems and the targeted designed catalysts with typical structural features is a meaningful subject, which deserves in-depth study to reveal the mechanisms of molecular evolution during the reaction process at high spatial resolution.



(2) Due to the electrocatalytic reaction involving multi-interaction between complicated active structures, the complementary detection from different orientations is necessary. Developing the methodologies for in-situ SR-FTIR in combination with a variety of other powerful instruments is recognized as a feasible concept to obtain more comprehensive information of molecular evolution during electrochemical reaction process. The available X-ray absorption fine structure (XAFS) technologies, which can track the dynamic evolution of local electronic structure, and high resolution transmission electron microscopic imaging technologies, which can display the lattice structure changes under operating conditions, are powerful tools for the underlying understanding of electrocatalytic mechanisms.

(3) The design of the optimal SR-FTIR setups and in-situ cells is of great importance for obtaining reliable data spectra, but still has a long way to go due to the lack of uniform and standardized design guidelines. Further efforts need to be invested in upgrading the SR-FTIR microscope and IR beam line, and minimizing the interference of the aqueous phase in the flow cell, etc. In the meanwhile, establishing a standard evaluation system for the installation and test parameters is urgently needed, so that the results of different tests can be compared. Moreover, quantitative SR-FTIR analysis should be considered by establishing functional relationships among various parameters, such as the species concentration as a function of the absorbance.

(4) The generation/cleavage of the new/old chemical bonds involved in the reaction process are completed rapidly in the micro-second order, which makes it a troublesome to vividly recount the lifetime evolution of reactive species. Time-resolved SR-FTIR spectroscopy, taking merits of the SR-based sources with pulse time resolutions up to microseconds or even nanoseconds, is attractive to provide a new perspective for clearer detection of active structures and reaction pathways. Thus, the development of cutting-edge time-resolved SR-FTIR spectroscopic techniques is a theoretically supported opportunity to capture the transient information of dynamic species, yet still faces enormous challenges.

## n ACKNOWLEDGEMENTS

This work was supported by the National Natural Science Foundation of China (Nos. 1932212, U1932109, 11875257).

## n AUTHOR INFORMATION

Corresponding authors. Emails: suhui@ustc.edu.cn and qhliu@ustc.edu.cn

## n COMPETING INTERESTS

The authors declare no competing interests.

## n ADDITIONAL INFORMATION

Full paper can be accessed via  
<http://manu30.magtech.com.cn/jghx/EN/10.14102/j.cnki.0254-5861.2022-0083>

For submission: <https://www.editorialmanager.com/cjschem>

## n REFERENCES

(1) Chu, S.; Majumdar, A. J. N. Opportunities and challenges for a sus-

tainable energy future. *Nature* **2012**, 488, 294-303.

(2) Sepulveda, N. A.; Jenkins, J. D.; Edington, A.; Mallapragada, D. S.; Lester, R. K. The design space for long-duration energy storage in decarbonized power systems. *Nat. Energy* **2021**, 6, 506-516.

(3) Feng, Y.; Tao, L.; Zheng, Z.; Huang, H.; Lin, F. Upgrading agricultural biomass for sustainable energy storage: bioprocessing, electrochemistry, mechanism. *Energy Storage Mater.* **2020**, 31, 274-309.

(4) Kang, S.; Miao, R.; Guo, J.; Fu, J. Sustainable production of fuels and chemicals from biomass over niobium based catalysts: a review. *Catal. Today* **2021**, 374, 61-76.

(5) Debe, M. K. Electrocatalyst approaches and challenges for automotive fuel cells. *Nature* **2012**, 486, 43-51.

(6) Stamenkovic, V. R.; Strmcnik, D.; Lopes, P. P.; Markovic, N. M. Energy and fuels from electrochemical interfaces. *Nat. Mater.* **2017**, 16, 57-69.

(7) Bu, L.; Zhang, N.; Guo, S.; Zhang, X.; Li, J.; Yao, J.; Wu, T.; Lu, G.; Ma, J.-Y.; Su, D. J. S. Biaxially strained PtPb/Pt core/shell nanoplate boosts oxygen reduction catalysis. *Science* **2016**, 354, 1410-1414.

(8) Zhou, W.; Su, H.; Wang, Z.; Yu, F.; Wang, W.; Chen, X.; Liu, Q. Self-synergistic cobalt catalysts with symbiotic metal single-atoms and nanoparticles for efficient oxygen reduction. *J. Mater. Chem. A* **2021**, 9, 1127-1133.

(9) Zhao, D.; Zhuang, Z.; Cao, X.; Zhang, C.; Peng, Q.; Chen, C.; Li, Y. D. Atomic site electrocatalysts for water splitting, oxygen reduction and selective oxidation. *Chem. Soc. Rev.* **2020**, 49, 2215-2264.

(10) Yang, H.; Han, X.; Douka, A. I.; Huang, L.; Gong, L.; Xia, C.; Park, H. S.; Xia, B. Y. Advanced oxygen electrocatalysis in energy conversion and storage. *Adv. Funct. Mater.* **2021**, 31, 2007602-2007630.

(11) Noguchi, H.; Okada, T.; Uosaki, K. Molecular structure at electrode/electrolyte solution interfaces related to electrocatalysis. *Faraday Discuss.* **2009**, 140, 125-137.

(12) Zhou, W.; Su, H.; Li, Y.; Liu, M.; Zhang, H.; Zhang, X.; Sun, X.; Xu, Y.; Liu, Q.; Wei, S. Identification of the evolving dynamics of coordination-unsaturated iron atomic active sites under reaction conditions. *ACS Energy Lett.* **2021**, 6, 3359-3366.

(13) Yang, Y.; Luo, M.; Zhang, W.; Sun, Y.; Chen, X.; Guo, S. J. Metal surface and interface energy electrocatalysis: fundamentals, performance engineering, and opportunities. *Chem* **2018**, 4, 2054-2083.

(14) Cai, W.; Chen, R.; Yang, H.; Tao, H. B.; Wang, H.-Y.; Gao, J.; Liu, W.; Liu, S.; Hung, S.-F.; Liu, B. Amorphous versus crystalline in water oxidation catalysis: a case study of NiFe alloy. *Nano Lett.* **2020**, 20, 4278-4285.

(15) Heidary, N.; Ly, K. H.; Kornienko, N. J. N. L. Probing CO<sub>2</sub> conversion chemistry on nanostructured surfaces with operando vibrational spectroscopy. *Nano Lett.* **2019**, 19, 4817-4826.

(16) Ting, L. R. L.; Yeo, B. S. Recent advances in understanding mechanisms for the electrochemical reduction of carbon dioxide. *Curr. Opin. Electrochem.* **2018**, 8, 126-134.

(17) Deng, Y. F.; Dong, S. Y.; Li, Z. F.; Jiang, H.; Zhang, X. G.; Ji, X. L. Applications of conventional vibrational spectroscopic methods for batteries beyond Li-ion. *Small Methods* **2018**, 2, 1700332-1700358.

(18) Zaera, F. Infrared and molecular beam studies of chemical reactions on solid surfaces. *Int. Rev. Phys. Chem.* **2002**, 21, 433-471.

(19) Li, Y.; Cheng, W.; Su, H.; Zhao, X.; He, J.; Liu, Q. Operando infrared spectroscopic insights into the dynamic evolution of liquid-solid (photo)electrochemical interfaces. *Nano Energy* **2020**, 77, 105121-105133.

(20) Zaera, F. New advances in the use of infrared absorption spectro-

- pscopy for the characterization of heterogeneous catalytic reactions.
- Chem. Soc. Rev.*
- 2014**
- , 43, 7624-7663.
- (21) Wang, H.; Zhou, Y.-W.; Cai, W.-B. Recent applications of in situ ATR-IR spectroscopy in interfacial electrochemistry. *Curr. Opin. Electrochem.* **2017**, 1, 73-79.
- (22) Andanson, J.-M.; Baiker, A. Exploring catalytic solid/liquid interfaces by in situ attenuated total reflection infrared spectroscopy. *Chem. Soc. Rev.* **2010**, 39, 4571-4584.
- (23) Hutter, E.; Assiongon, K.; Fendler, J.; Roy, D. Fourier transform infrared spectroscopy using polarization modulation and polarization selective techniques for internal and external reflection geometries: investigation of self-assembled octadecylmercaptan on a thin gold film. *J. Phys. Chem. B* **2003**, 107, 7812-7819.
- (24) Petit, T.; Puskar, L. FTIR spectroscopy of nanodiamonds: methods and interpretation. *Diamond Relat. Mater.* **2018**, 89, 52-66.
- (25) Duncan, W.; Williams, G. P. Infrared synchrotron radiation from electron storage rings. *Appl. Opt.* **1983**, 22, 2914-2923.
- (26) Singley, E.; Abo-Bakr, M.; Basov, D.; Feikes, J.; Guptasarma, P.; Holldack, K.; Hübers, H.; Kuske, P.; Martin, M. C.; Peatman, W. Measuring the Josephson plasma resonance in  $\text{Bi}_2\text{Sr}_2\text{CaCu}_2\text{O}_8$  using intense coherent THz synchrotron radiation. *Phys. Rev. B* **2004**, 69, 092512-092515.
- (27) Hu, C. S.; Wang, X.; Qi, Z. M.; Li, C. X. The new infrared beamline at NSRL. *Infrared Phys. Technol.* **2020**, 105, 103200-103204.
- (28) Su, H.; Zhou, W.; Zhang, H.; Zhou, W.; Zhao, X.; Li, Y.; Liu, M.; Cheng, W.; Liu, Q. Dynamic evolution of solid-liquid electrochemical interfaces over single-atom active sites. *J. Am. Chem. Soc.* **2020**, 142, 12306-12313.
- (29) Hirschmugl, C.; Williams, G. Signal-to-noise improvements with a new far-IR rapid scan Michelson interferometer. *Rev. Sci. Instrum.* **1995**, 66, 1487-1488.
- (30) Marcelli, A.; Cricenti, A.; Kwiatek, W. M.; Petibois, C. Biological applications of synchrotron radiation infrared spectromicroscopy. *Biotechnol. Adv.* **2012**, 30, 1390-1404.
- (31) Nichols, E. F. A study of the transmission spectra of certain substances in the infra-red. *Phys. Rev. (Series I)* **1893**, 1, 1-18.
- (32) Coates, V. J.; Offner, A.; Siegler, E. Design and performance of an infrared microscope attachment. *J. Opt. Soc. Am.* **1953**, 43, 984-989.
- (33) Golden, W. G.; Saperstein, D. D. Phenomena, R. Fourier transform infrared reflection-absorption spectroscopy of surface species. *J. Electron. Spectrosc. Relat. Phenom.* **1983**, 30, 43-50.
- (34) Sherma, J. Fourier transform infrared (FT-IR) spectrometry. *J. AOAC Int.* **2004**, 87, 113A-118A.
- (35) Mattson, E. C.; Nasse, M. J.; Rak, M.; Gough, K. M.; Hirschmugl, C. J. Restoration and spectral recovery of mid-infrared chemical images. *Anal. Chem.* **2012**, 84, 6173-6180.
- (36) Greenler, R. G. Infrared study of adsorbed molecules on metal surfaces by reflection techniques. *J. Chem. Phys.* **1966**, 44, 310-315.
- (37) Roy, P.; Brubach, J.-B.; Calvani, P.; DeMarzi, G.; Filabozzi, A.; Gerschel, A.; Giura, P.; Lupi, S.; Marcouillé, O.; Mermet, A. Infrared synchrotron radiation: from the production to the spectroscopic and microscopic applications. *Nucl. Instrum. Methods Phys. Res., Sect. A* **2001**, 467, 426-436.
- (38) Hirschmugl, C. Infrared synchrotron radiation instrumentation and applications. *Nucl. Instrum. Methods Phys. Res. Sect. A* **1992**, 319, 245-249.
- (39) Stavitski, E.; Kox, M. H.; Swart, I.; de Groot, F. M.; Weckhuysen, B. M. In situ synchrotron-based IR microspectroscopy to study catalytic reactions in zeolite crystals. *Angew. Chem. Int. Ed.* **2008**, 120, 3599-3603.
- (40) Buurmans, I. L.; Soulimani, F.; Ruiz-Martínez, J.; Van Der Bij, H. E.; Weckhuysen, B. M. Structure and acidity of individual fluid catalytic cracking catalyst particles studied by synchrotron-based infrared micro-spectroscopy. *Microporous Mesoporous Mater.* **2013**, 166, 86-92.
- (41) Dumas, P.; Jamin, N.; Teillaud, J.; Miller, L.; Beccard, B. Imaging capabilities of synchrotron infrared microspectroscopy. *Faraday Discuss.* **2004**, 126, 289-302.
- (42) Kovar, M.; Kasza, R.; Griffiths, K.; Norton, P.; Williams, G.; Van Campen, D. Synchrotron radiation FTIR spectroscopic studies of water on Ni(110). *Surf. Rev. Lett.* **1998**, 5, 589-598.
- (43) Li, X.; Yang, X.; Zhang, J.; Huang, Y.; Liu, B. In situ/operando techniques for characterization of single-atom catalysts. *ACS Catal.* **2019**, 9, 2521-2531.
- (44) Carr, G. Resolution limits for infrared microspectroscopy explored with synchrotron radiation. *Rev. Sci. Instrum.* **2001**, 72, 1613-1619.
- (45) Levenson, E.; Lerch, P.; Martin, M. C. Spatial resolution limits for synchrotron-based spectromicroscopy in the mid- and near-infrared. *J. Synchrotron Radiat.* **2008**, 15, 323-328.
- (46) Lobo, R.; LaVeigne, J.; Reitze, D.; Tanner, D.; Carr, G. Subnanosecond, time-resolved, broadband infrared spectroscopy using synchrotron radiation. *Rev. Sci. Instrum.* **2002**, 73, 1-10.
- (47) Zhang, Y.; Zhang, H.; Liu, A.; Chen, C.; Song, W.; Zhao, J. Rate-limiting O-O bond formation pathways for water oxidation on hematite photoanode. *J. Am. Chem. Soc.* **2018**, 140, 3264-3269.
- (48) Chittur, K. K. FTIR/ATR for protein adsorption to biomaterial surfaces. *Biomaterials* **1998**, 19, 357-369.
- (49) Martin, M. C.; Schade, U.; Lerch, P.; Dumas, P. Recent applications and current trends in analytical chemistry using synchrotron-based Fourier-transform infrared microspectroscopy. *TrAC, Trends Anal. Chem.* **2010**, 29, 453-463.
- (50) Dumas, P.; Miller, L.; Tobin, M. Challenges in biology and medicine with synchrotron infrared light. *Acta Phys. Pol.* **2009**, 115, 446-454.
- (51) Eischens, R.; Pliskin, W. The infrared spectra of adsorbed molecules. *Adv. Catal.* **1958**, 10, 1-56.
- (52) Willey, R. Fourier transform infrared spectrophotometer for transmittance and diffuse reflectance measurements. *Appl. Spectrosc.* **1976**, 30, 593-601.
- (53) Mudunkotuwa, I. A.; Al Minshid, A.; Grassian, V. H. ATR-FTIR spectroscopy as a tool to probe surface adsorption on nanoparticles at the liquid-solid interface in environmentally and biologically relevant media. *Analyst* **2014**, 139, 870-881.
- (54) Hoffmann, F. Infrared reflection-absorption adsorbed molecules spectroscopy. *Surf. Sci. Rep.* **1983**, 3, 107-192.
- (55) Miki, A.; Ye, S.; Osawa, M. Surface-enhanced IR absorption on platinum nanoparticles: an application to real-time monitoring of electrocatalytic reactions. *Chem. Commun.* **2002**, 1500-1501.
- (56) Nayak, S.; McPherson, I. J.; Vincent, K. A. Adsorbed intermediates in oxygen reduction on platinum nanoparticles observed by in situ IR spectroscopy. *Angew. Chem. Int. Ed.* **2018**, 57, 12855-12858.
- (57) Zaera, F. New advances in the use of infrared absorption spectroscopy for the characterization of heterogeneous catalytic reactions. *Chem. Soc. Rev.* **2014**, 43, 7624-7663.
- (58) Ortiz-Hernandez, I.; Williams, C. T. In situ investigation of solid-liquid catalytic interfaces by attenuated total reflection infrared spectroscopy. *Langmuir* **2003**, 19, 2956-2962.

- (59) Kan, B.-C.; Boo, J.-H.; Lee, I.; Zaera, F. Thermal chemistry of tetrakis (ethylmethylamido) titanium on Si (100) surfaces. *J. Phys. Chem. A* **2009**, 113, 3946-3954.
- (60) Kaim, W.; Fiedler, J. Spectroelectrochemistry: the best of two worlds. *Chem. Soc. Rev.* **2009**, 38, 3373-3382.
- (61) Cheng, W.; Zhao, X.; Su, H.; Tang, F.; Che, W.; Zhang, H.; Liu, Q. Lattice-strained metal-organic-framework arrays for bifunctional oxygen electrocatalysis. *Nat. Energy* **2019**, 4, 115-122.
- (62) Lv, C.; Zhong, L.; Liu, H.; Fang, Z.; Yan, C.; Chen, M.; Kong, Y.; Lee, C.; Liu, D.; Li, S.; Liu, J.; Song, L.; Chen, G.; Yan, Q.; Yu, G. Selective electrocatalytic synthesis of urea with nitrate and carbon dioxide. *Nat. Sustain.* **2021**, 4, 868-876.
- (63) Dionigi, F.; Zeng, Z.; Sinev, I.; Merzdorf, T.; Deshpande, S.; Lopez, M. B.; Kunze, S.; Zegkinoglou, I.; Sarodnik, H.; Fan, D. In-situ structure and catalytic mechanism of NiFe and CoFe layered double hydroxides during oxygen evolution. *Nat. Commun.* **2020**, 11, 1-10.
- (64) Su, H.; Soldatov, M. A.; Roldugin, V.; Liu, Q. Platinum single-atom catalyst with self-adjustable valence state for large-current-density acidic water oxidation. *eScience* **2022**, 2, 102-109.
- (65) Jiao, Y.; Zheng, Y.; Jaroniec, M.; Qiao, S. Z. Design of electrocatalysts for oxygen- and hydrogen-involving energy conversion reactions. *Chem. Soc. Rev.* **2015**, 44, 2060-2086.
- (66) Yin, Q.; Tan, J. M.; Besson, C.; Geletii, Y. V.; Musaev, D. G.; Kuznetsov, A. E.; Luo, Z.; Hardcastle, K. I.; Hill, C. L. A fast soluble carbon-free molecular water oxidation catalyst based on abundant metals. *Science* **2010**, 328, 342-345.
- (67) Zhang, X.; Sun, X.; Li, Y.; Hu, F.; Xu, Y.; Tian, J.; Zhang, H.; Liu, Q.; Su, H.; Wei, S. Reduced interfacial tension on ultrathin NiCr-LDH nanosheet arrays for efficient electrocatalytic water oxidation. *J. Mater. Chem. A* **2021**, 9, 16706-16712.
- (68) Gloag, L.; Benedetti, T. M.; Cheong, S.; Li, Y.; Chan, X. H.; Lacroix, L. M.; Chang, S. L. Y.; Arenal, R.; Florea, I.; Barron, H.; Barnard, A. S.; Henning, A. M.; Zhao, C.; Schuhmann, W.; Gooding, J. J.; Tilley, R. D. Three-dimensional branched and faceted gold-ruthenium nanoparticles: using nanostructure to improve stability in oxygen evolution electrocatalysis. *Angew. Chem. Int. Ed.* **2018**, 57, 10241-10245.
- (69) Su, H.; Zhao, X.; Cheng, W.; Zhang, H.; Li, Y.; Zhou, W.; Liu, M.; Liu, Q. Hetero-N-coordinated Co single sites with high turnover frequency for efficient electrocatalytic oxygen evolution in an acidic medium. *ACS Energy Lett.* **2019**, 4, 1816-1822.
- (70) Lin, C.; Li, J.-L.; Li, X.; Yang, S.; Luo, W.; Zhang, Y.; Kim, S.-H.; Kim, D.-H.; Shinde, S. S.; Li, Y.-F.; Liu, Z.-P.; Jiang, Z.; Lee, J.-H. In-situ reconstructed Ru atom array on  $\alpha$ -MnO<sub>2</sub> with enhanced performance for acidic water oxidation. *Nat. Catal.* **2021**, 4, 1012-1023.
- (71) Zhao, X.; Su, H.; Cheng, W.; Zhang, H.; Che, W.; Tang, F.; Liu, Q. Operando insight into the oxygen evolution kinetics on the metal-free carbon-based electrocatalyst in an acidic solution. *ACS Appl. Mater. Interfaces* **2019**, 11, 34854-34861.
- (72) Cao, L.; Luo, Q.; Chen, J.; Wang, L.; Lin, Y.; Wang, H.; Liu, X.; Shen, X.; Zhang, W.; Liu, W.; Qi, Z.; Jiang, Z.; Yang, J.; Yao, T. Dynamic oxygen adsorption on single-atomic ruthenium catalyst with high performance for acidic oxygen evolution reaction. *Nat. Commun.* **2019**, 10, 4849-4857.
- (73) Su, H.; Zhou, W.; Zhou, W.; Li, Y.; Zheng, L.; Zhang, H.; Liu, M.; Zhang, X.; Sun, X.; Xu, Y.; Hu, F.; Zhang, J.; Hu, T.; Liu, Q.; Wei, S. In-situ spectroscopic observation of dynamic-coupling oxygen on atomically dispersed iridium electrocatalyst for acidic water oxidation. *Nat. Commun.* **2021**, 12, 6118-6126.
- (74) Zhang, Q.; Guan, J. Applications of atomically dispersed oxygen reduction catalysts in fuel cells and zinc-air batteries. *Energy Environ. Mater.* **2020**, 4, 307-335.
- (75) Zhou, W.; Su, H.; Shen, S.; Li, Y.; Zhang, H.; Liu, M.; Zhao, X.; Cheng, W.; Yao, P.; Liu, Q. Co-Ni nanoalloy-organic framework electrocatalysts with ultrahigh electron transfer kinetics for efficient oxygen reduction. *ACS Sustainable Chem. Eng.* **2020**, 8, 6898-6904.
- (76) Zhou, Z.; Kong, Y.; Tan, H.; Huang, Q.; Wang, C.; Pei, Z.; Wang, H.; Liu, Y.; Wang, Y.; Li, S.; Liao, X.; Yan, W.; Zhao, S. Cation-vacancy-enriched nickel phosphide for efficient electrosynthesis of hydrogen peroxides. *Adv. Mater.* **2022**, e2106541.
- (77) Liu, M.; Li, Y.; Qi, Z.; Su, H.; Cheng, W.; Zhou, W.; Zhang, H.; Sun, X.; Zhang, X.; Xu, Y.; Jiang, Y.; Liu, Q.; Wei, S. Self-nanocavity-confined halogen anions boosting the high selectivity of the two-electron oxygen reduction pathway over Ni-based MOFs. *J. Phys. Chem. Lett.* **2021**, 12, 8706-8712.
- (78) Ke, K.; Wang, G.; Cao, D.; Wang, G. J. E. Recent advances in the electrooxidation of urea for direct urea fuel cell and urea electrolysis. *Top. Curr. Chem.* **2020**, 41-78.
- (79) Sayed, E. T.; Eisa, T.; Mohamed, H. O.; Abdelkareem, M. A.; Allagui, A.; Alawadhi, H.; Chae, K.-J. Direct urea fuel cells: challenges and opportunities. *J. Power Sources* **2019**, 417, 159-175.
- (80) Geng, S.-K.; Zheng, Y.; Li, S.-Q.; Su, H.; Zhao, X.; Hu, J.; Shu, H.-B.; Jaroniec, M.; Chen, P.; Liu, Q.-H.; Qiao, S.-Z. Nickel ferrocyanide as a high-performance urea oxidation electrocatalyst. *Nat. Energy* **2021**, 6, 904-912.
- (81) Service, R. F. New recipe produces ammonia from air, water, and sunlight. *Science* **2014**, 345, 610.
- (82) Giddey, S.; Badwal, S.; Kulkarni, A. Review of electrochemical ammonia production technologies and materials. *Int. J. Hydrogen Energy* **2013**, 38, 14576-14594.
- (83) Tan, H.; Ji, Q.; Wang, C.; Duan, H.; Kong, Y.; Wang, Y.; Feng, S.; Lv, L.; Hu, F.; Zhang, W.; Chu, W.; Sun, Z.; Yan, W. Asymmetrical  $\pi$  back-donation of hetero-dicationic Mo<sup>4+</sup>-Mo<sup>6+</sup> pairs for enhanced electrochemical nitrogen reduction. *Nano Res.* **2021**, 15, 3010-3016.
- (84) Chen, C.; Zhu, X.; Wen, X.; Zhou, Y.; Zhou, L.; Li, H.; Tao, L.; Li, Q.; Du, S.; Liu, T.; Yan, D.; Xie, C.; Zou, Y.; Wang, Y.; Chen, R.; Huo, J.; Li, Y.; Cheng, J.; Su, H.; Zhao, X.; Cheng, W.; Liu, Q.; Lin, H.; Luo, J.; Chen, J.; Dong, M.; Cheng, K.; Li, C.; Wang, S. Coupling N<sub>2</sub> and CO<sub>2</sub> in H<sub>2</sub>O to synthesize urea under ambient conditions. *Nat. Chem.* **2020**, 12, 717-724.
- (85) Li, C.; Baek, J.-B. Recent advances in noble metal (Pt, Ru, and Ir)-based electrocatalysts for efficient hydrogen evolution reaction. *ACS Omega* **2019**, 5, 31-40.
- (86) Mahmood, J.; Li, F.; Jung, S.-M.; Okyay, M. S.; Ahmad, I.; Kim, S.-J.; Park, N.; Jeong, H. Y.; Baek, J.-B. An efficient and pH-universal ruthenium-based catalyst for the hydrogen evolution reaction. *Nat. Nanotech.* **2017**, 12, 441-446.
- (87) Li, Y.; He, J.; Cheng, W.; Su, H.; Li, C.; Zhang, H.; Liu, M.; Zhou, W.; Chen, X.; Liu, Q. High mass-specific reactivity of a defect-enriched Ru electrocatalyst for hydrogen evolution in harsh alkaline and acidic media. *Sci. China Mater.* **2021**, 64, 2467-2476.
- (88) Zhang, H.; Su, H.; Soldatov, M. A.; Li, Y.; Zhao, X.; Liu, M.; Zhou, W.; Zhang, X.; Sun, X.; Xu, Y.; Yao, P.; Wei, S.; Liu, Q. Dynamic CoRu bond shrinkage at atomically dispersed Ru sites for alkaline hydrogen evolution reaction. *Small* **2021**, 17, 2105231-2105237.

(89) He, Q.; Zhou, Y.; Shou, H.; Wang, X.; Zhang, P.; Xu, W.; Qiao, S.; Wu, C.; Liu, H.; Liu, D.; Chen, S.; Long, R.; Qi, Z.; Wu, X.; Song, L. Synergic reaction kinetics over adjacent ruthenium sites for superb hydrogen generation in alkaline media. *Adv. Mater.* **2022**, e2110604.

(90) Cao, D.; Sheng, B.; Qi, Z.; Xu, W.; Chen, S.; Moses, O. A.; Long, R.; Xiong, Y.; Wu, X.; Song, L. Self-optimizing iron phosphorus oxide for stable hydrogen evolution at high current. *Appl. Catal., B* **2021**, 298, 120559-120566.

(91) Li, N.; Tan, H.; Ding, X.; Duan, H.; Hu, W.; Li, G.; Ji, Q.; Lu, Y.; Wang,

Y.; Hu, F.; Wang, C.; Cheng, W.; Sun, Z.; Yan, W. Phase-mediated robust interfacial electron-coupling over core-shell Co@carbon towards superior overall water splitting. *Appl. Catal., B* **2020**, 266, 118621-118627.

Received: April 12, 2022

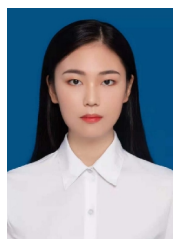
Accepted: April 30, 2022

Published online: May 12, 2022

Published: October 25, 2022



**Wanlin Zhou** received her B.S. degree from the Northeastern University in June 2018. She is currently studying for her Ph.D. degree at University of Science and Technology of China (USTC). Her current research focuses on the design and characterization of electrocatalysts for industrial energy storage and conversion technologies. She specializes in tracing the local structure evolution and catalytic dynamics of heterogeneous catalytic interfaces by using in-situ synchrotron radiation XAS and FTIR techniques.



**Jingjing Jiang** received her B.S. degree from the Anhui University in June 2021. She is currently studying for a doctorate at University of Science and Technology of China under the supervision of Prof. Shiqiang Wei and Prof. Qinghua Liu. Her current research focuses on the design and synthesis of energy conversion nanomaterials and advanced in situ/operando synchrotron radiation experimental techniques.



**Weiren Cheng** received his Ph.D. degree from the University of Science and Technology of China (USTC) in June 2015, and is a member of National Synchrotron Radiation Laboratory, USTC, and a foreign researcher in Hokkaido University, Japan, now. He currently interests in the design and synthesis of advanced functional nanomaterials for energy-related applications as well as the understanding of their catalytic mechanisms by *in-situ* synchrotron techniques.



**Hui Su** received his B.S. degree from the Hefei University of Technology in June 2015 and Ph.D. degree from the University of Science and Technology of China (USTC) in June 2020, and is a member of National Synchrotron Radiation Laboratory, USTC. His current research focuses on engineering nanoscale catalysts at the atomic scale to enable high efficiency renewable energy conversion, and probing and understanding of nanoscale catalysts dynamic structure evolution at solid-liquid interface for reaction kinetics studies by operando synchrotron radiation XAS & FTIR techniques.



**Qinghua Liu** is currently a doctoral supervisor of National Synchrotron Radiation Laboratory, University of Science and Technology of China (USTC). He received his Ph.D. in 2009 from USTC and subsequently performed research work on renewable energy conversion and synchrotron radiation experimental techniques. His current research interests focus on the synthesis and characterization of advanced energy functional nanomaterials for photocatalytic, electrochemical, and photoelectrochemical applications and the development of advanced *in situ/operando* synchrotron radiation experimental techniques and their applications in energy storage and reaction mechanisms.